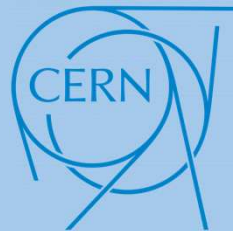


Study of SPNDs irradiation at NEAR-nTOF (CERN): Data analysis



UNIVERSIDAD
DE GRANADA

Juan Antonio Moreno
Antonio Pousibet Garrido
Alberto J. Palma, ajpalma@ugr.es
Miguel Ángel Carvajal, carvajal@ugr.es



Salvatore Fiore
Ana-Paula Bernardes
Marco Calviani

Ciemat

Santiago Becerril
Rafael Vila

Who we are?

Multidisciplinary research group since 2000:

Engineers: Electronics, ICT and Computer Science

Scientifics: Chemists and Physicists

Lab. technicians.

Our general goal:

The design, development and fabrication of sensors, microfluidic devices and portable instrumentation for analysis and monitoring with application in various areas.

Our experience in radiation detection systems:

- MOSFET dosimetry systems based on general purpose transistors and RADFETs
- Electrometers for general purpose diodes and photodiodes.



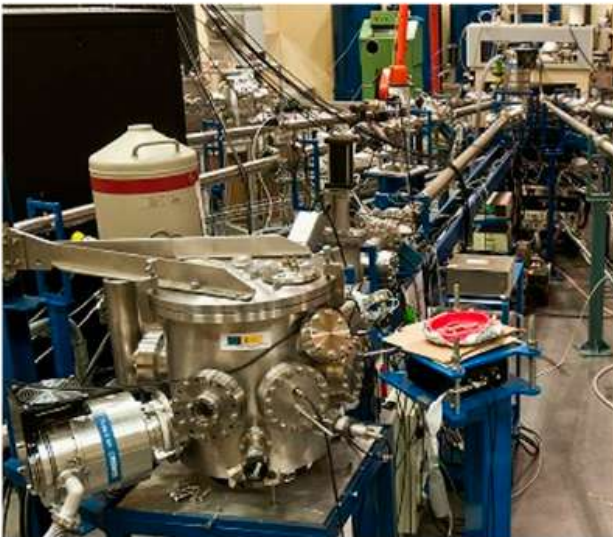
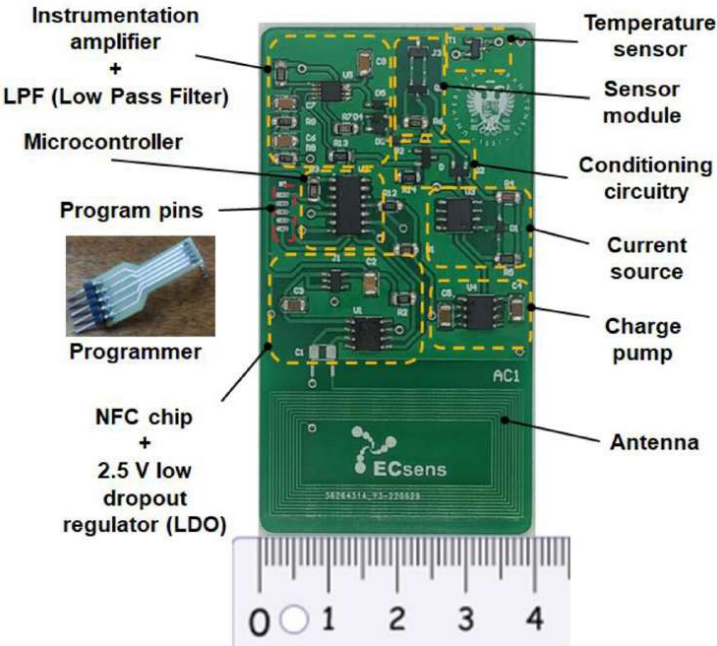
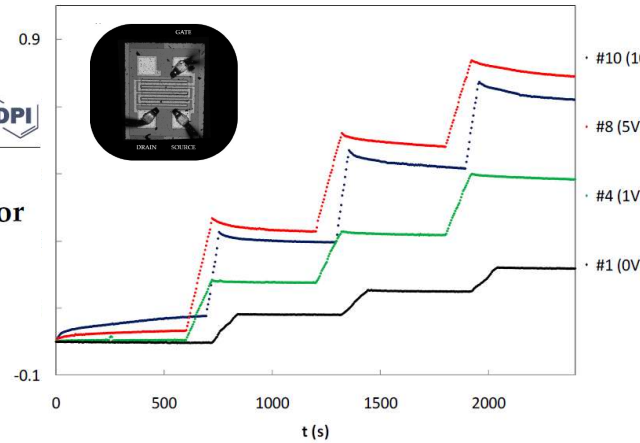
Who we are?

Our experience in radiation detection systems:



Article
General Purpose Transistor Characterized as Dosimetry Sensor of Proton Beams

J. A. Moreno-Pérez ¹, I. Ruiz-García ¹, P. Martín-Holgado ², A. Romero-Maestre ², M. Anguiano ³, R. Vila ⁴ and M. A. Carvajal ^{1,*}



Irradiation chamber
 MOSFET reader unit
 PC to remote control



Contents lists available at [ScienceDirect](https://www.sciencedirect.com)

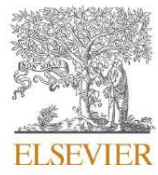
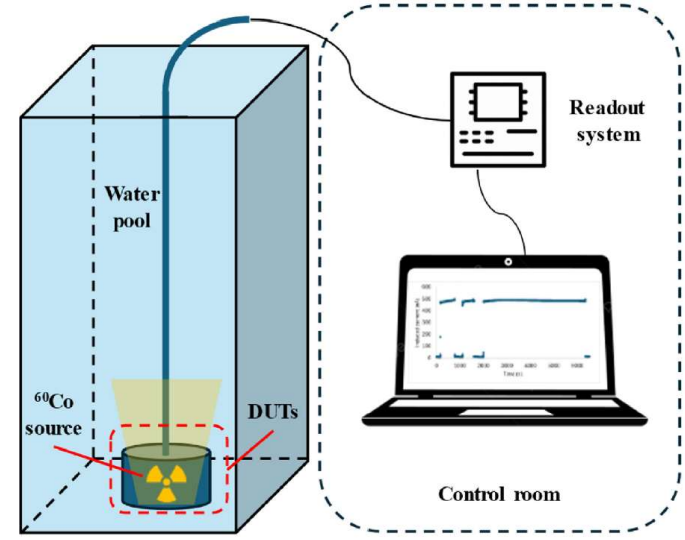
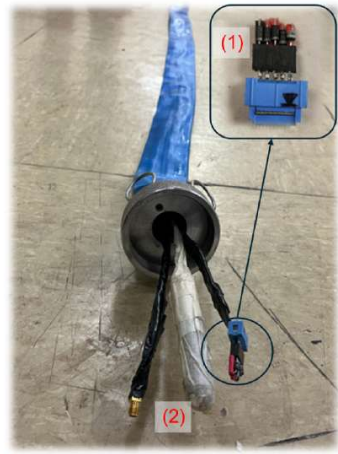
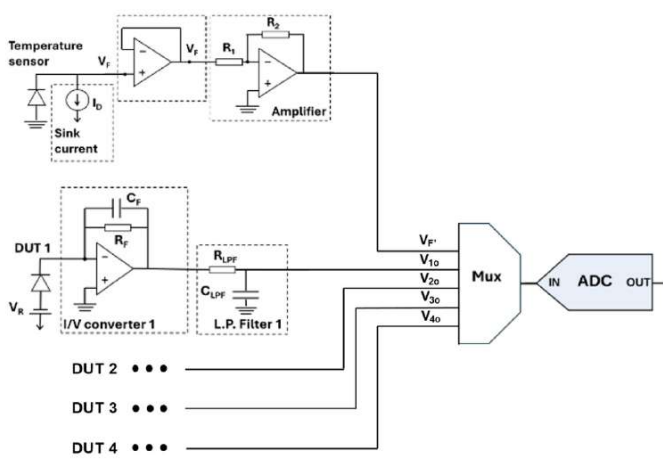
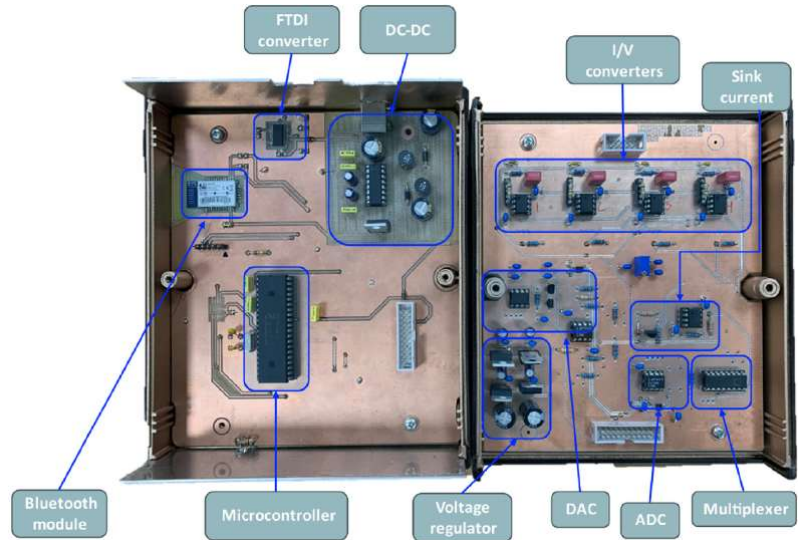
Sensors and Actuators: A. Physical

journal homepage: www.journals.elsevier.com/sensors-and-actuators-a-physical

Batteryless NFC dosimeter tag for ionizing radiation based on commercial MOSFET

A. Pousibet-Garrido ^a, P. Escobedo ^a, D. Guirado ^{b,c}, G.S. Ristic ^d, A.J. Palma ^a, M.A. Carvajal ^{a,*}

Who we are?



Contents lists available at ScienceDirect

Radiation Physics and Chemistry

journal homepage: www.elsevier.com/locate/radphyschem

High dose-rate gamma radiation response of commercial off-the-shelf diodes

I. Ruiz-García^a, J.A. Moreno-Pérez^a, P. Valdivieso^b, P. Escobedo^a, A.J. Palma^a, R. Vila^c, M.A. Carvajal^{a,*}



Who we are?

(2) **CNA (Sevilla): TANDEM Accelerator**
5.36 MeV Protons

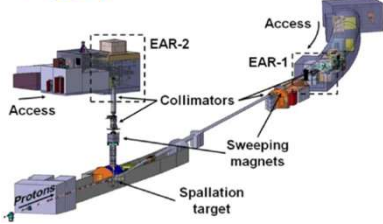



Extracted from:
<https://cna.us.es/index.php/es/instalaciones/tandem>

(3) **CIEMAT (Madrid): NAYADE Facility**
Co-60 Source




(4) **CERN (Switzerland): n_TOF Facility**
Pulsed neutron beam



<https://doi.org/10.1051/epjconf/202430401009>

(1) **CIBM-UGR (Granada): Comet Yxlon X-ray Source**
Photons (X-ray Spectrum)



(5) **PSI (Switzerland): PIF Facility**
70-230 MeV Protons



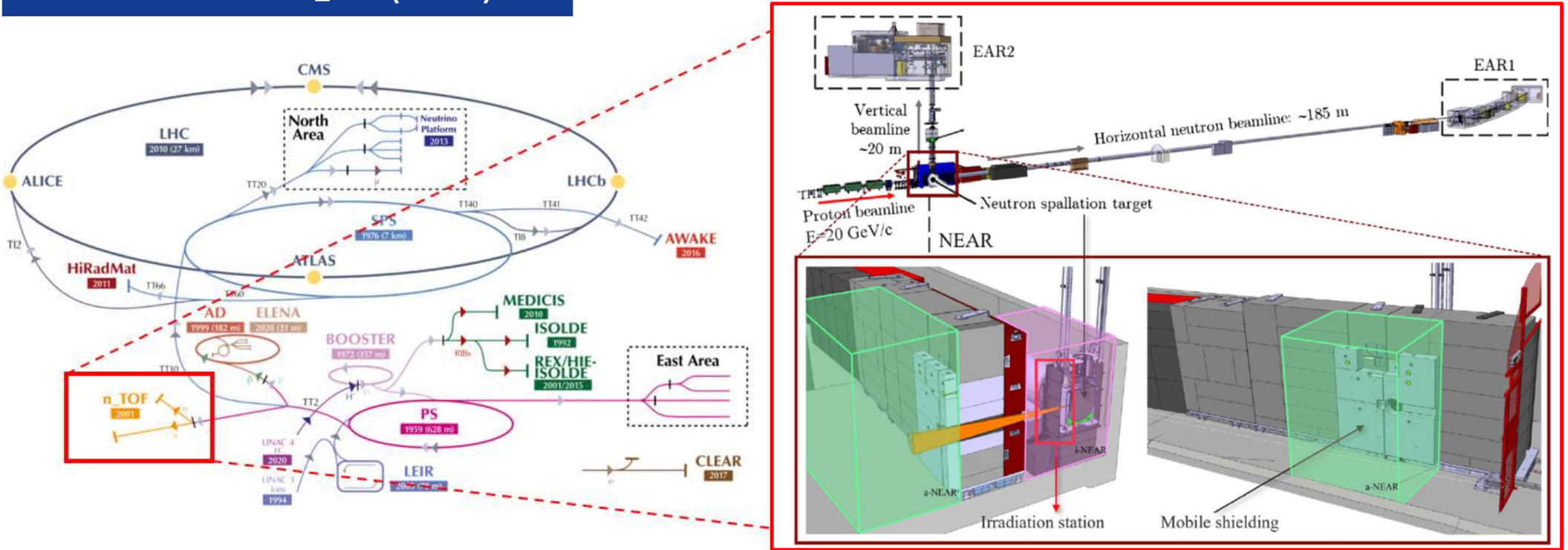
Extracted from: <https://www.psi.ch/en/pif>

Study of SPNDs irradiation at NEAR-nTOF (CERN): Data analysis

1. Experimental Setup
2. Delayed response analysis
3. Prompt response analysis
5. Conclusions and future tasks

1. Experimental Setup

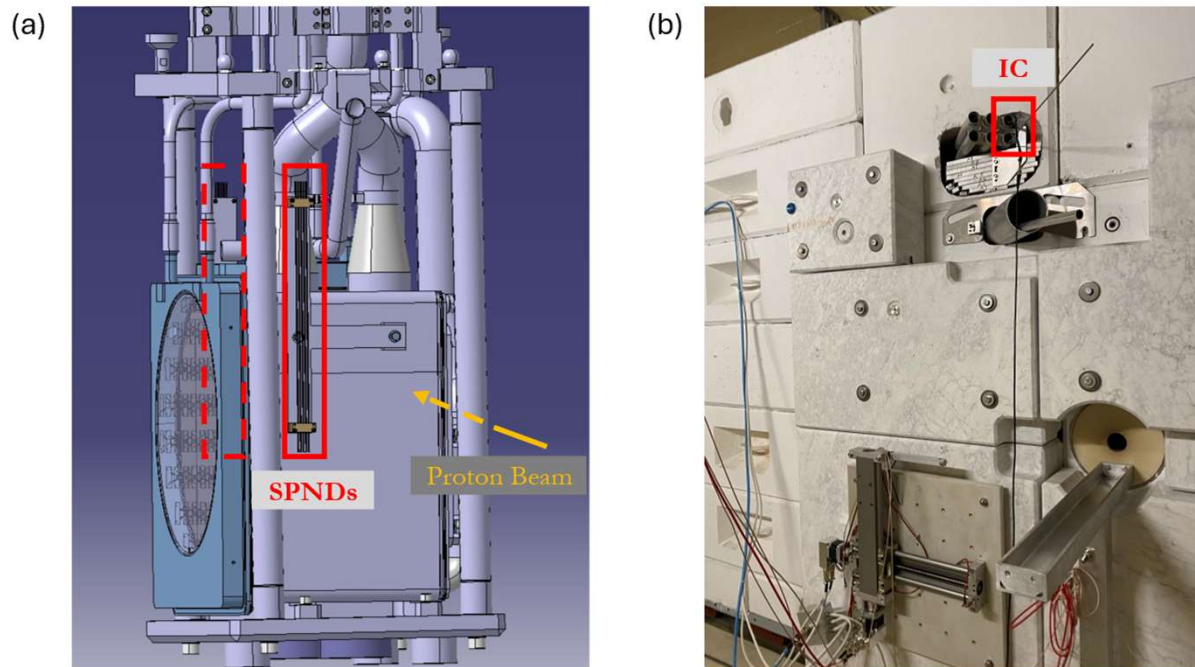
NEAR Station – n_TOF (CERN)



The SPNDs were placed at the NEAR station, in both sides of the target, one of each emitter material. Proton pulses of 30 ns reach the target with varying intensities and patterns every 1.2 seconds or multiples thereof.

1. Experimental Setup

NEAR Station – n_TOF (CERN)



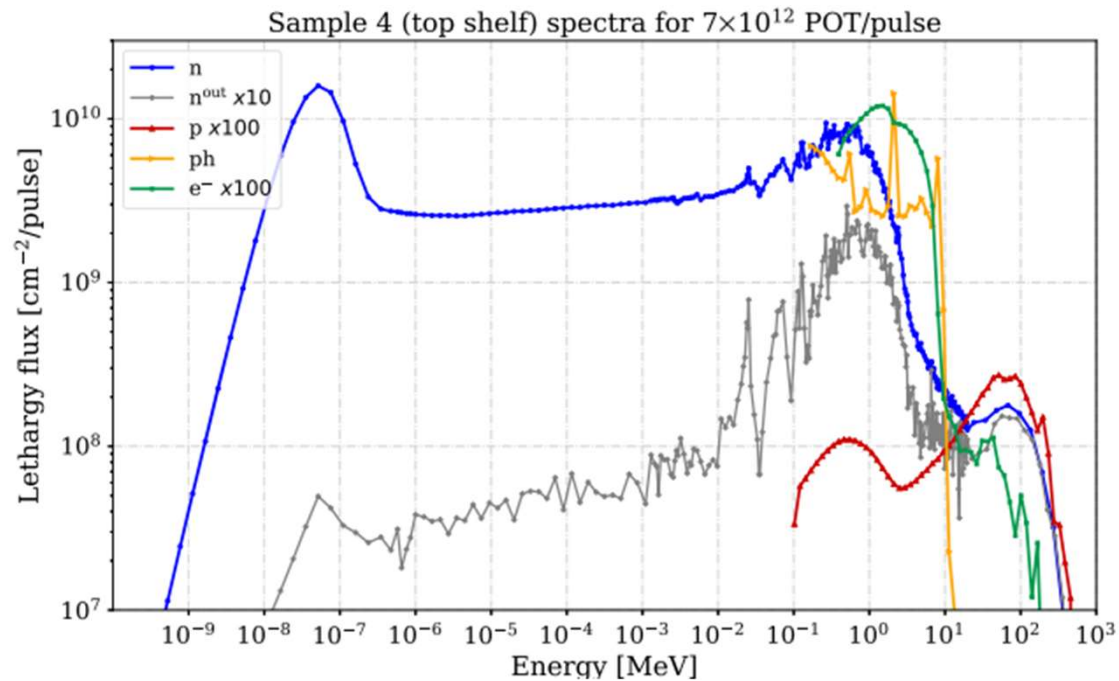
Location of the detectors: (a) SPNDs inside the target area (i-NEAR); (b) IC inside a rabbit tube (a-NEAR)

The SPNDs were placed at the NEAR station, in both sides of the target, one of each emitter material.

Proton pulses of 30 ns reach the target with varying intensities and patterns every 1.2 seconds or multiples thereof.

1. Experimental Setup

Particle spectrum

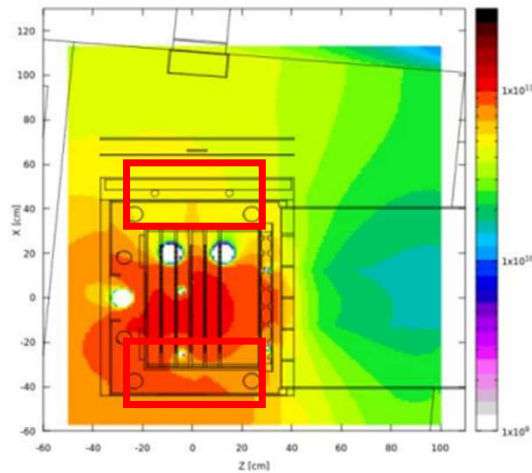


M. Ferrari et al., Design development and implementation of an irradiation station at the neutron time-of-flight facility at CERN, *Physical Review Accelerators And Beams* 25, 103001 (2022)
DOI: 10.1103/PhysRevAccelBeams.25.103001

1. Experimental Setup

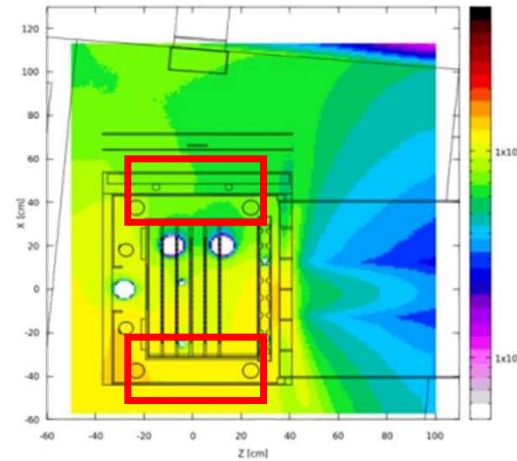
Simulations of radiation conditions for the approximate position of the SPNDs

NEUTRON DISTRIBUTION ($n/cm^2/pulse$)



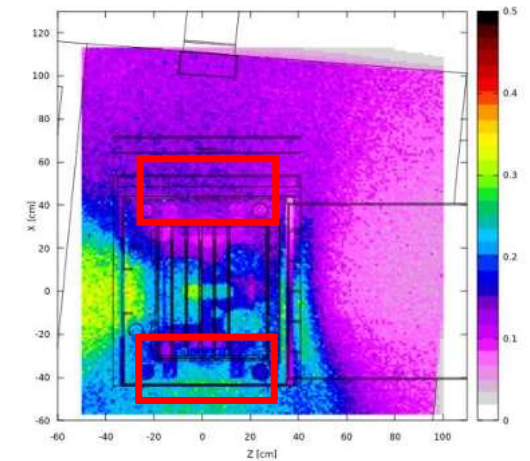
- Left side: $\sim 6 \times 10^{10}$ $n/cm^2/pulse$
- Right side: $\sim 10 \times 10^{10}$ $n/cm^2/pulse$

GAMMA DISTRIBUTION ($\gamma/cm^2/pulse$)



- Left side: $\sim 6.5 \times 10^9$ $\gamma/cm^2/pulse$
- Right side: $\sim 1.2 \times 10^{10}$ $\gamma/cm^2/pulse$

PROMPT DOSE (Gy/pulse)

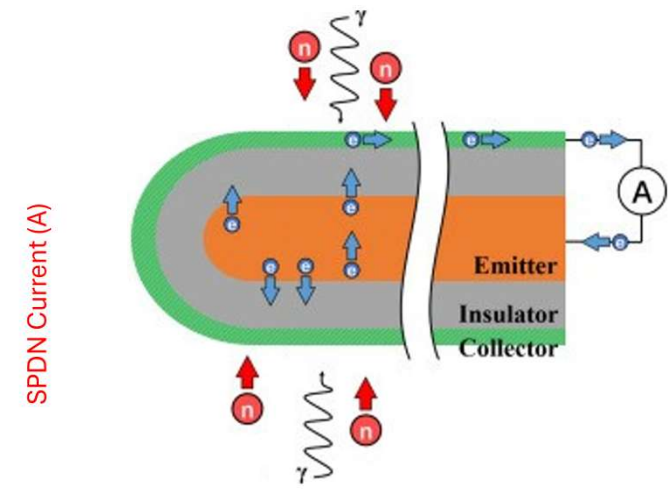
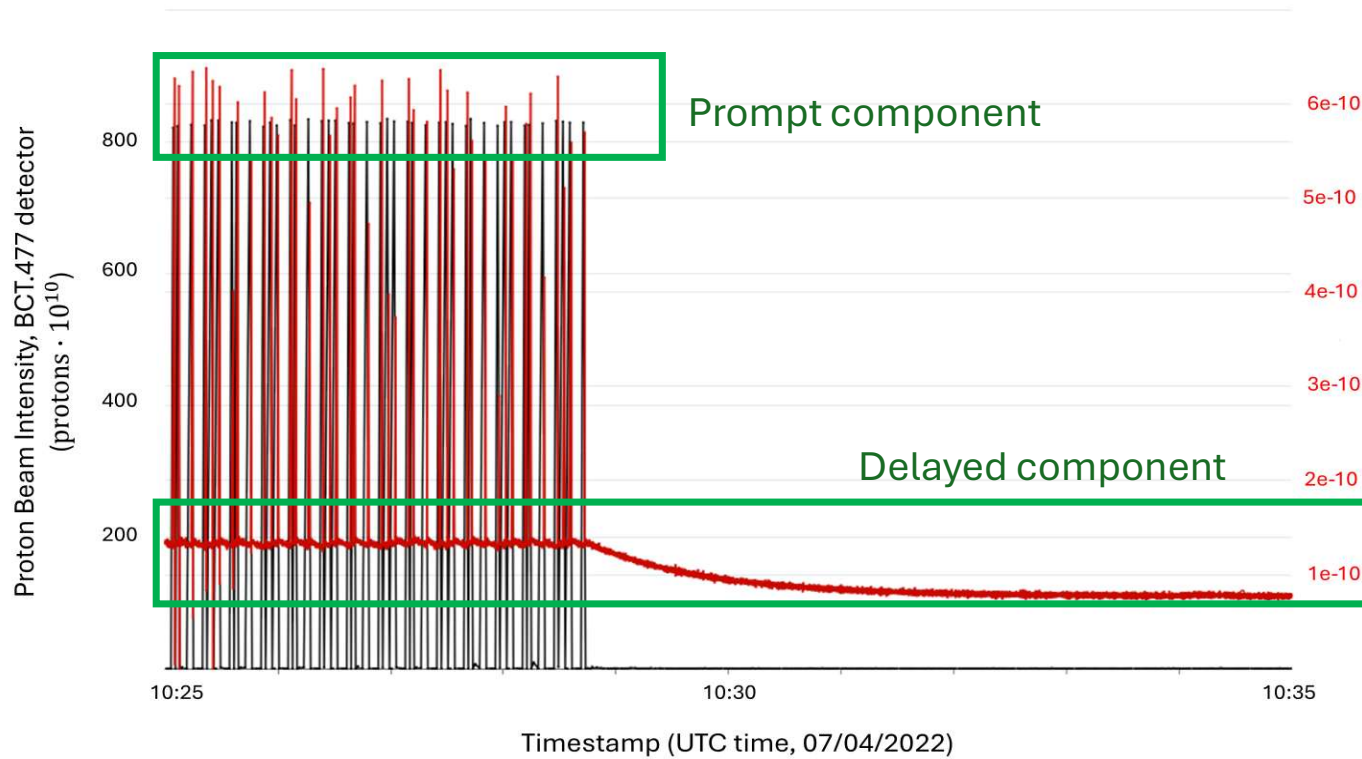


- Left side: ~ 0.1 Gy/pulse
- Right side: ~ 0.2 Gy/pulse

Left side ~ 50 % of the right side measurements.

Simulations of the radiation conditions made by M. Barbagallo, V. Vlachoudis, Mattei Cecchetto

1. Experimental Setup



Tongyuan Cui et al., (2020)

1. Experimental Setup

Emitter material	Isotopes	Response type (mainly)	Half-life time
Rhodium (Rh)	$^{103}\text{Rh} - ^{104}\text{Rh}$	Delayed	42.3 s
Cobalt (Co)	$^{59}\text{Co} - ^{60}\text{Co}$	Prompt	5.27 yr
Platinum (Pt)	$^{195}\text{Pt} - ^{197}\text{Pt}$	Prompt	-
Vanadium (V)	$^{51}\text{V} - ^{52}\text{V}$	Delayed	3.8 min
Inconel (In)	Employed as a “dummy” detector, with the same collector and emitter materials, to subtract the background from the neutron component of the signal.		

2. Delayed Response Analysis: Half-life

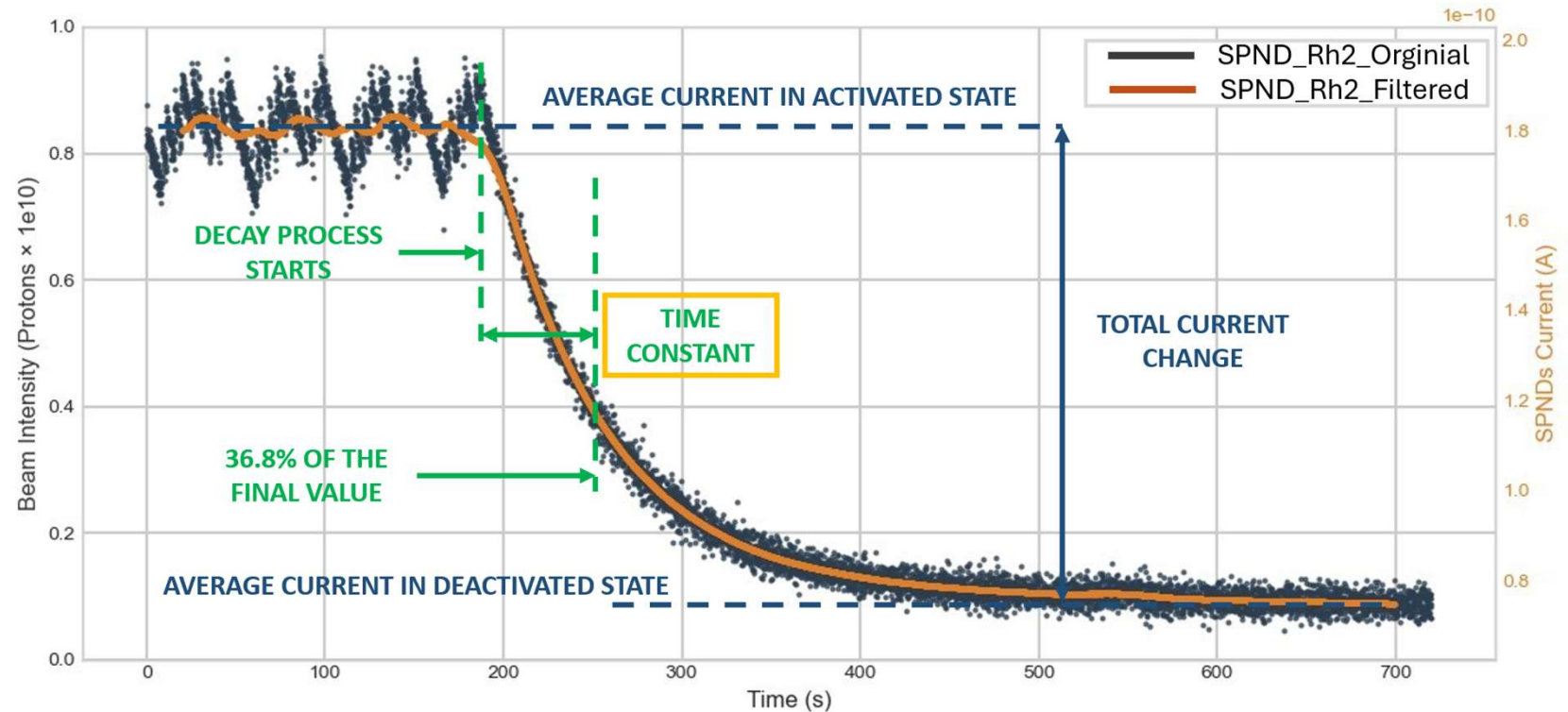
Delayed component analysis: Half-life

Moving window median filter applied to the original current measurements.

The **time constant** of the exponential response was determined: **63.2%** of the final value during **activation** and **36.8%** during **decay**.

The **time constant (τ)** is related to the **half-life ($t_{1/2}$)**:

$$t_{1/2} = \ln(2) \cdot \tau$$



2. Delayed Response Analysis: Half-life



Main conclusion of 2024 analysis: **Detectors were mislabelled.**

Label in NXCALS	Real material
V_1	Rh_1
Co_2	Rh_2
Rh_1	V_1
Ch_12	V_2
Pt_1	Co_1
Rh_2	Co_2
Co_1	Pt_1
In_1	Pt_2
Pt_2	In_1
Ch_11	In_2

2. Delayed Response Analysis: Half-life

Delayed component analysis: Half-life

Only the **Rh and V detectors** exhibit a **delayed component** that is appreciable within the time scale studied. **Pt detectors** may show a noticeable delayed response on a time scale of **approximately 20 hours**, whereas **Co detectors** would not exhibit such behavior until several years have passed (**approximately 5–6 years**).

Detector material	Decay				Activation				Avg. Half-life (s)	
	03/11/2021		12/04/2022		03/11/2021		12/04/2022		Avg	SD
	τ (s)	Half-life (s)	τ (s)	Half-life (s)	τ (s)	Half-life (s)	τ (s)	Half-life (s)		
Rh_1	73	50	64	44	81	56	87	60	53	7
Rh_2	74	51	64	44	81	56	88	61	53	7
V_1	284	197	329	228	346	240	293	203	217	20
V_2	296	205	344	238	339	235	305	211	223	17

Activation processes showed longer times due to the pulsed nature of the beam.

The half-lives obtained are:

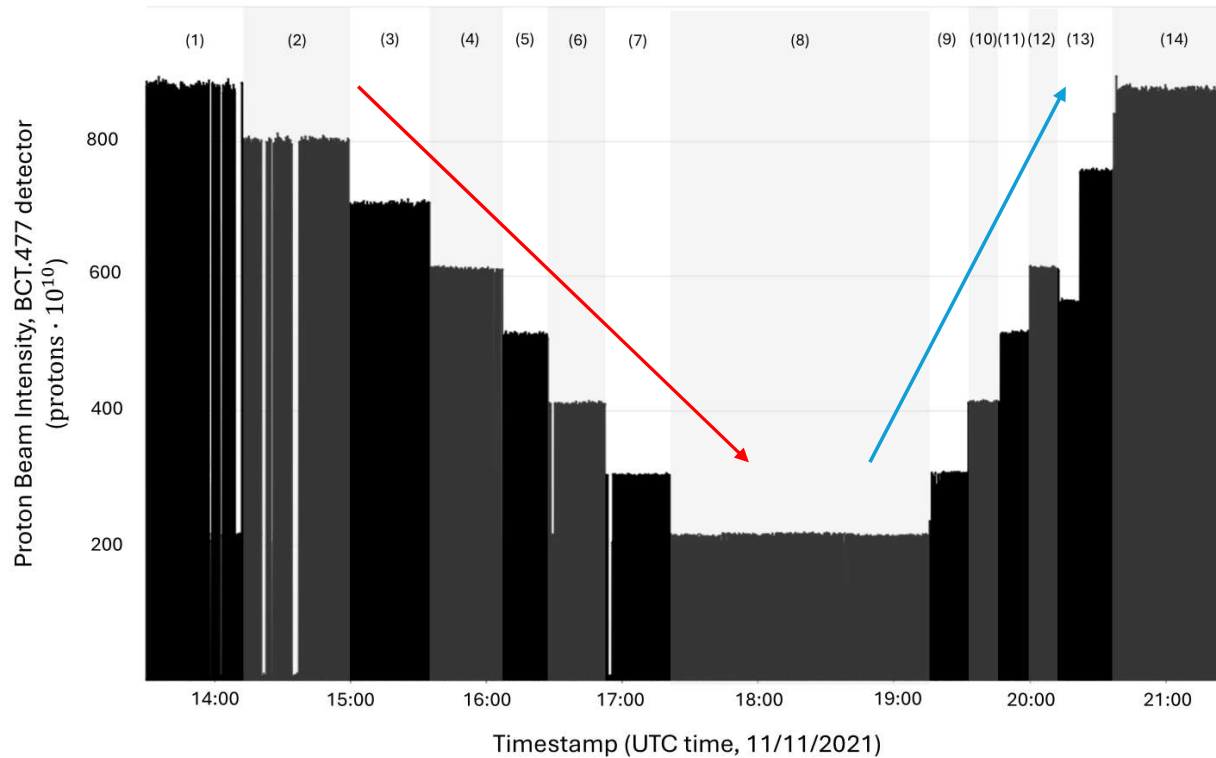
- **Rh detectors ~53 s (ideal 43.2 s)**
- **V detectors ~ 3.7 min (ideal 3.7 min)**



Gives an estimation on **how fast** the detectors can **respond to the changes in the flux through (n, β) reactions.**

2. Delayed Response Analysis: Sensitivity

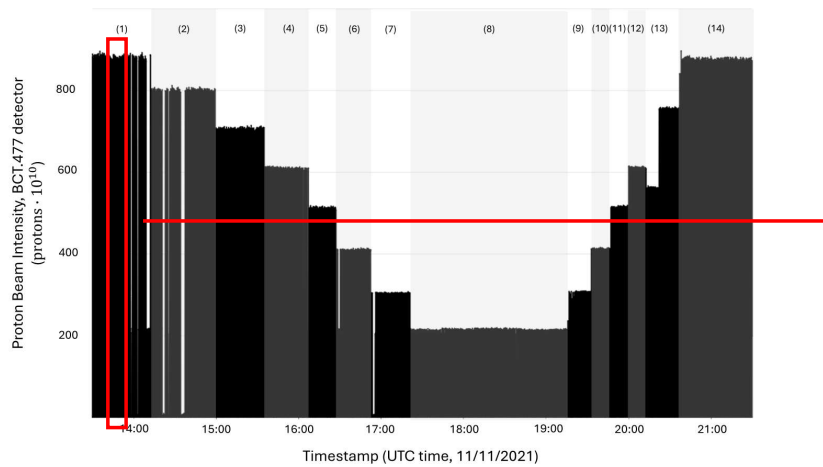
Delayed component analysis: Linearity with the proton flux



On 11/11/2021, pulses of different intensities and patterns were generated, based on measurements from the BCT.477 detector. The **delayed response** was measured under **14 different beam conditions** to **evaluate the linearity** of the response. The **analysis** was **divided** into two parts: **decreasing intensity (1-8)** and **increasing intensity (8-14)**.

2. Delayed Response Analysis: Sensitivity

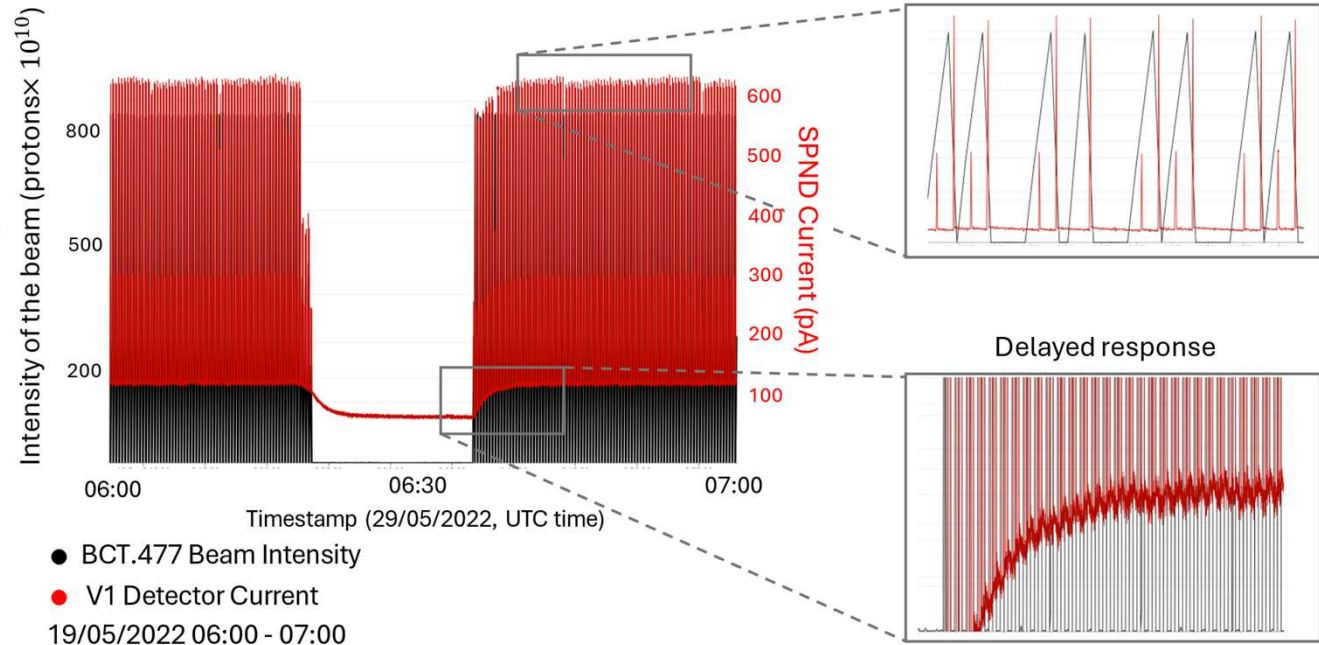
Delayed component analysis: Linearity with the proton flux



Since there is no direct reference for the neutron conditions, the BCT.477, which measures the proton flux reaching the target, is taken as the reference.

To perform the analysis:

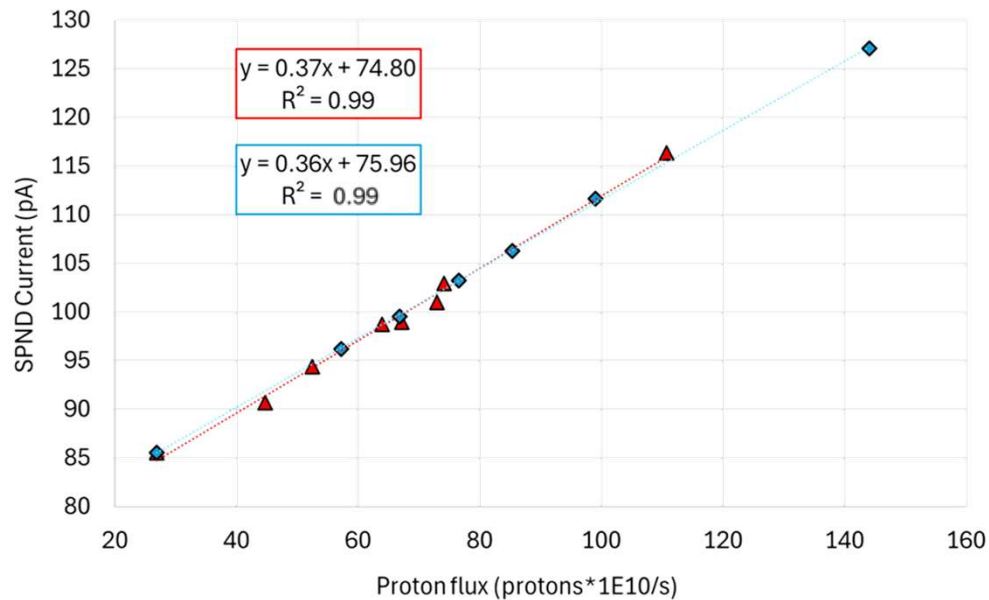
- (1) For each beam intensity, approximately **one full cycle** of the proton beam pattern (lasting **between 30 and 120 seconds**, depending on the case) was considered.
- (2) The **peaks** of the detector's signal, which **correspond to the prompt response**, were **subtracted from the baseline**.
- (3) The **average proton flux for each cycle** was obtained by summing the proton count over time and dividing by the duration of the cycle.
- (4) **After a stabilization period** of about 10–20 minutes, the **baseline average** was compared to the **average proton flux** during that cycle.



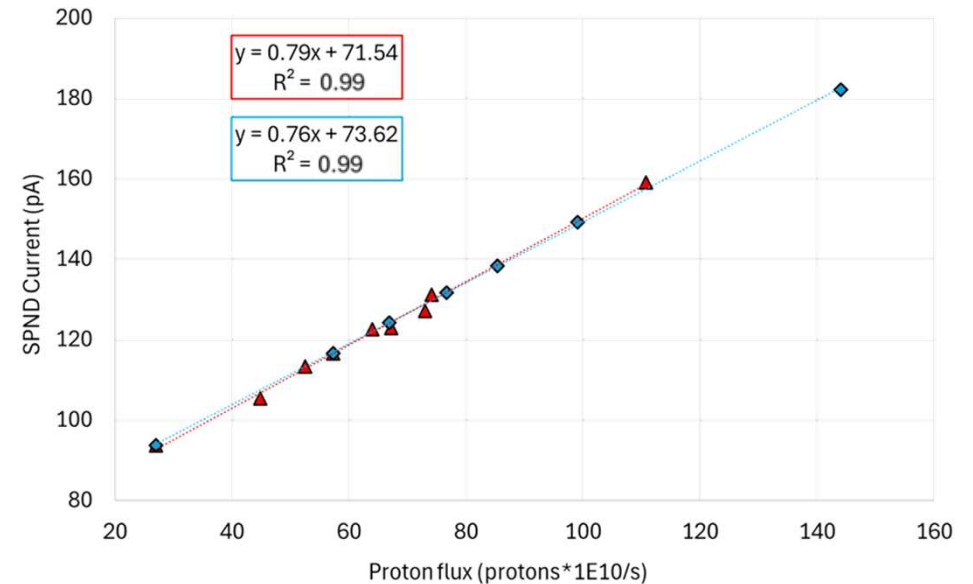
2. Delayed Response Analysis: Sensitivity

Delayed component analysis: rhodium detectors

Rh_1 Detector



Rh_2 Detector



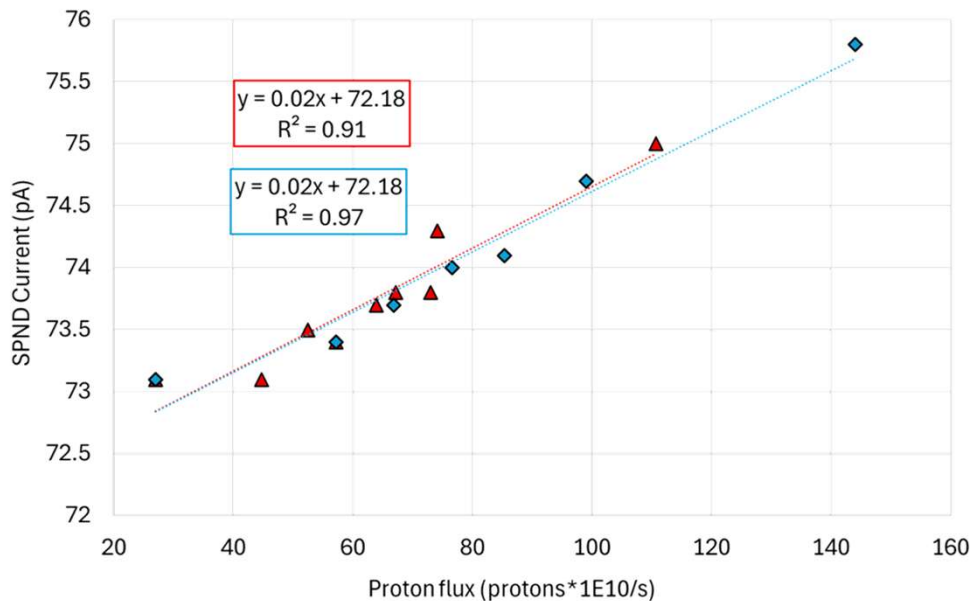
Detectors show **high linearity** with respect to the proton flux ($R^2 = 0.99$), with **sensitivities** of **0.36-0.37 pA/(p· 10¹⁰/s)** in the left position and **0.76-0.79 pA/(p· 10¹⁰/s)** in the right position.

The sensitivity of the **Rh_1 detector** is **47.24%** of the signal of the **Rh_2 detector**.

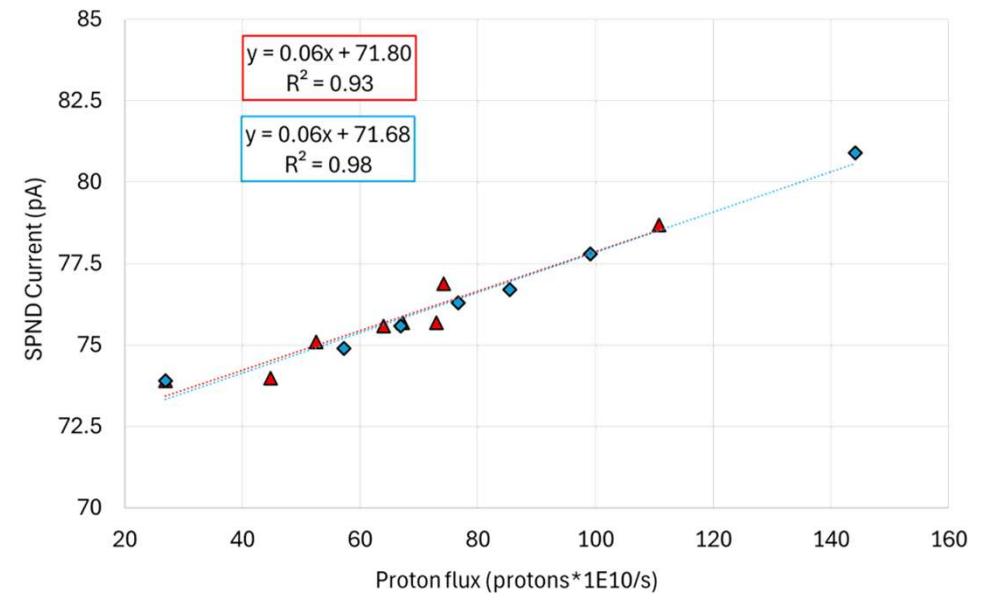
3. Delayed Response Analysis: Sensitivity

Delayed component analysis: vanadium detectors

V_1 Detector



V_2 Detector



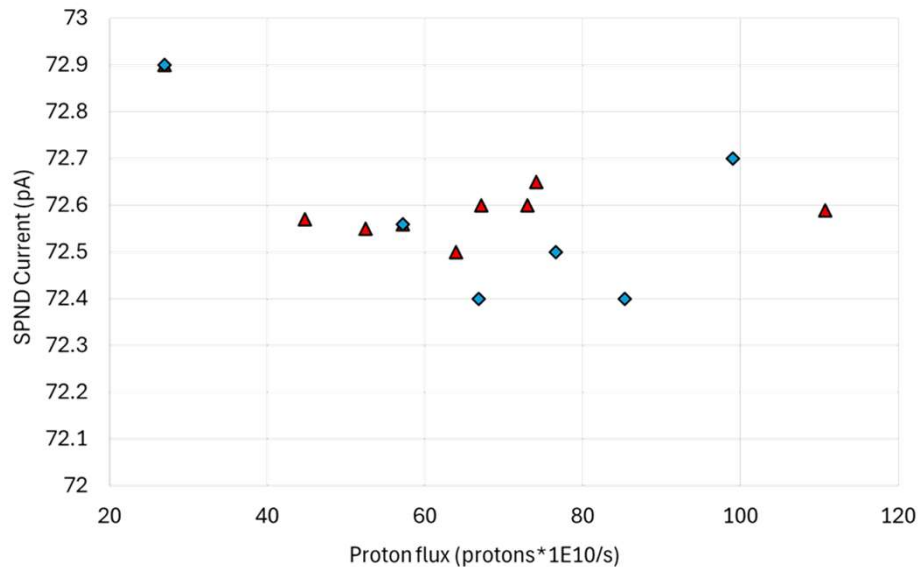
Detectors show **high linearity** with respect to the proton flux ($R^2 \approx 0.91 - 0.98$), with **sensitivities of 0.02 pA/(p·10¹⁰/s) in the left position and 0.06 pA/(p·10¹⁰/s) in the right position.**

The sensitivity of the **V_1 detector** is **33.3%** of the signal of the **V_2 detector**.

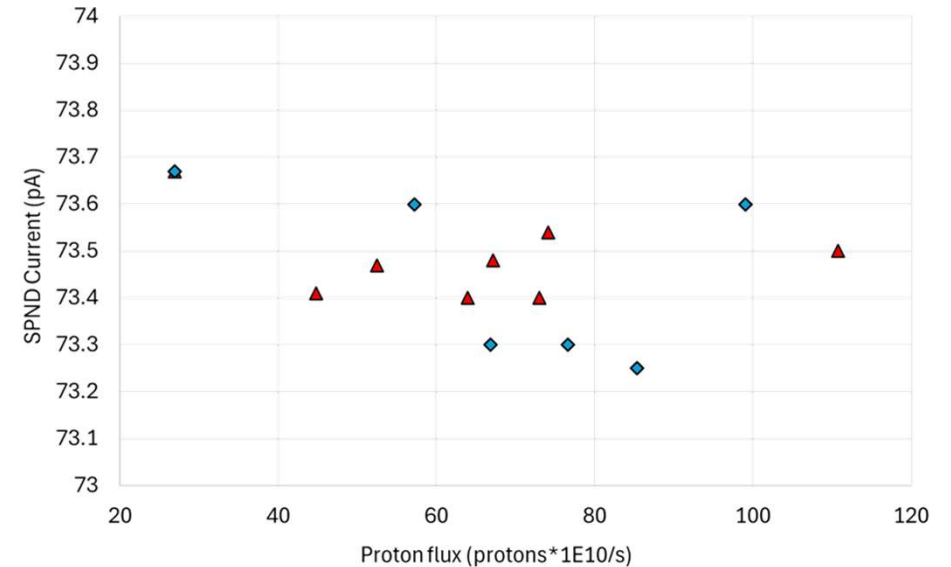
3. Delayed Response Analysis: Sensitivity

Delayed component analysis: platinum detectors

Pt_1 Detector



Pt_2 Detector

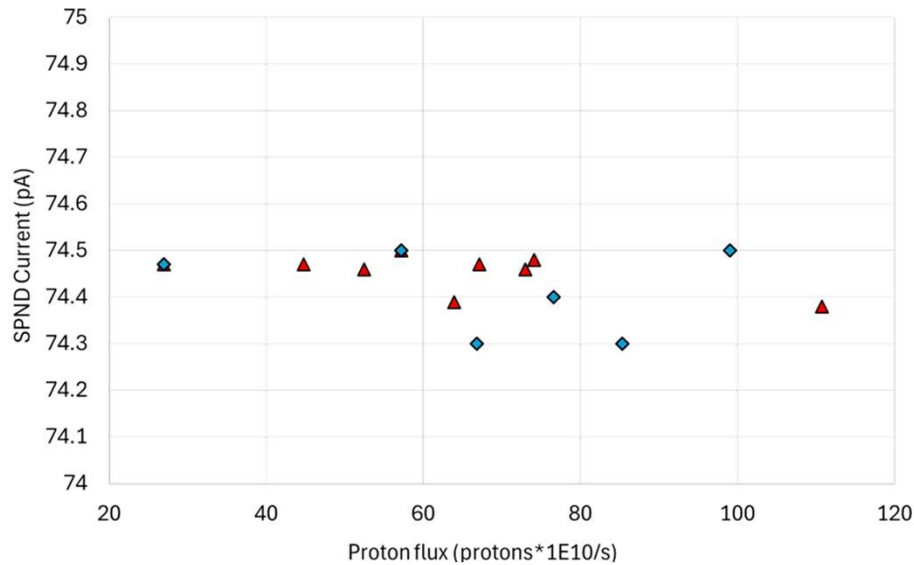


The **proton flux does not appear to influence the delayed response of the platinum detectors**, with an **average current of 72.58 ± 0.12 pA** for the **left-position detector** and **73.47 ± 0.14 pA** for the **right-position detector**.

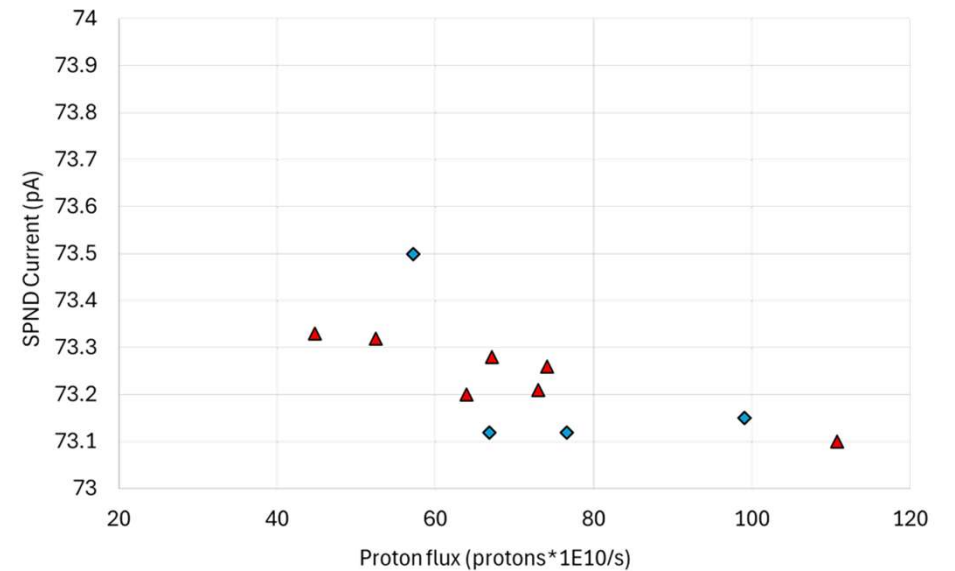
3. Delayed Response Analysis: Sensitivity

Delayed component analysis: cobalt detectors

Co_1 Detector



Co_2 Detector

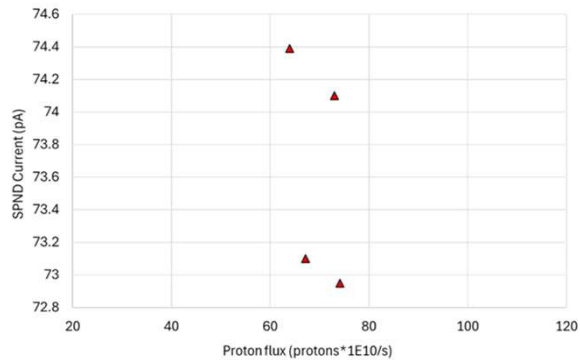
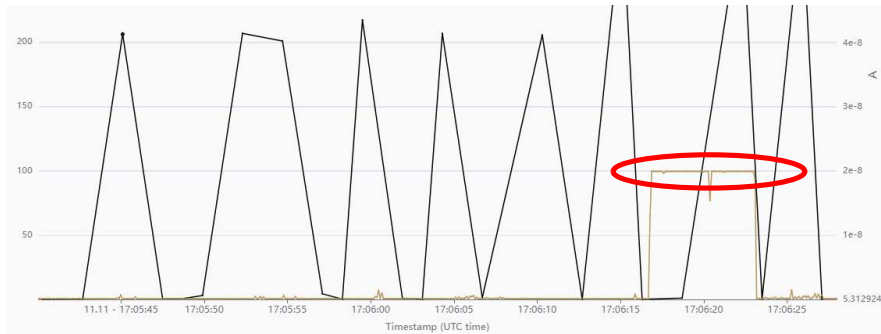


The proton flux does not appear to influence the response of the cobalt detectors, with an average current of 74.42 ± 0.08 pA for the left-position detector and 73.27 ± 0.28 pA for the right-position detector.

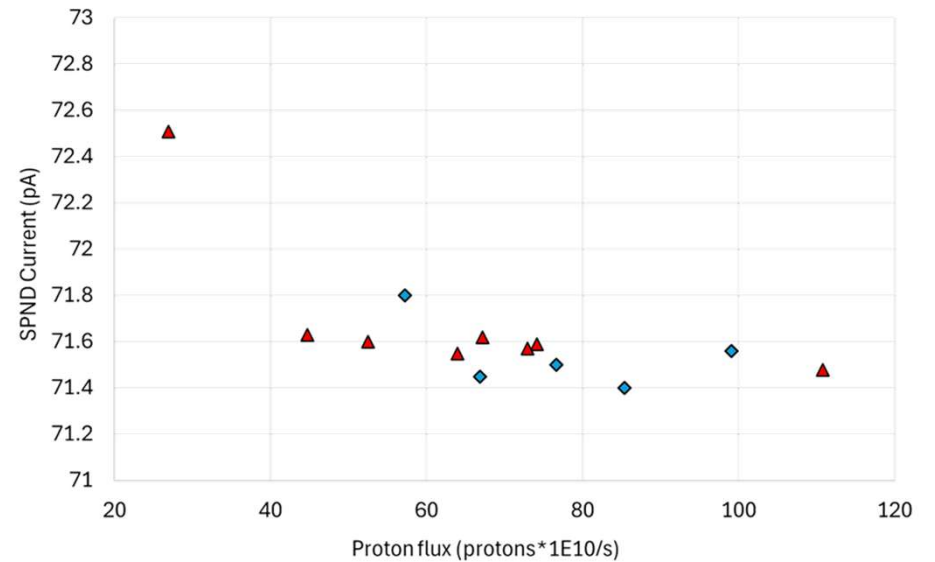
3. Delayed Response Analysis: Sensitivity

Delayed component analysis: inconel detectors

In_1 Detector



In_2 Detector



Only a few values of the **In_1 detector** are considered, since it had a **strange behaviour** during this date. The **proton flux does not appear to influence the response of the inconel detectors**, with an **average current of 73.6 ± 0.7 pA for the left-position detector and 71.6 ± 0.3 pA for the right-position detector.**

3. Delayed Response Analysis: Sensitivity

Delayed component analysis: summary

Detector	Appreciable Delayed Response Observed During the Studied Time Interval?	Sensitivity to the proton flux (pA/(p · 10 ¹⁰ /s))	Half-life (s)
Rh_1	Yes	0.36-0.37	53
Rh_2	Yes	0.76-0.79	53
V_1	Yes	0.02	217
V_2	Yes	0.06	223
Co_1	No	-	-
Co_2	No	-	-
Pt_1	No	-	-
Pt_2	No	-	-
In_1	No	-	-
In_2	No	-	-

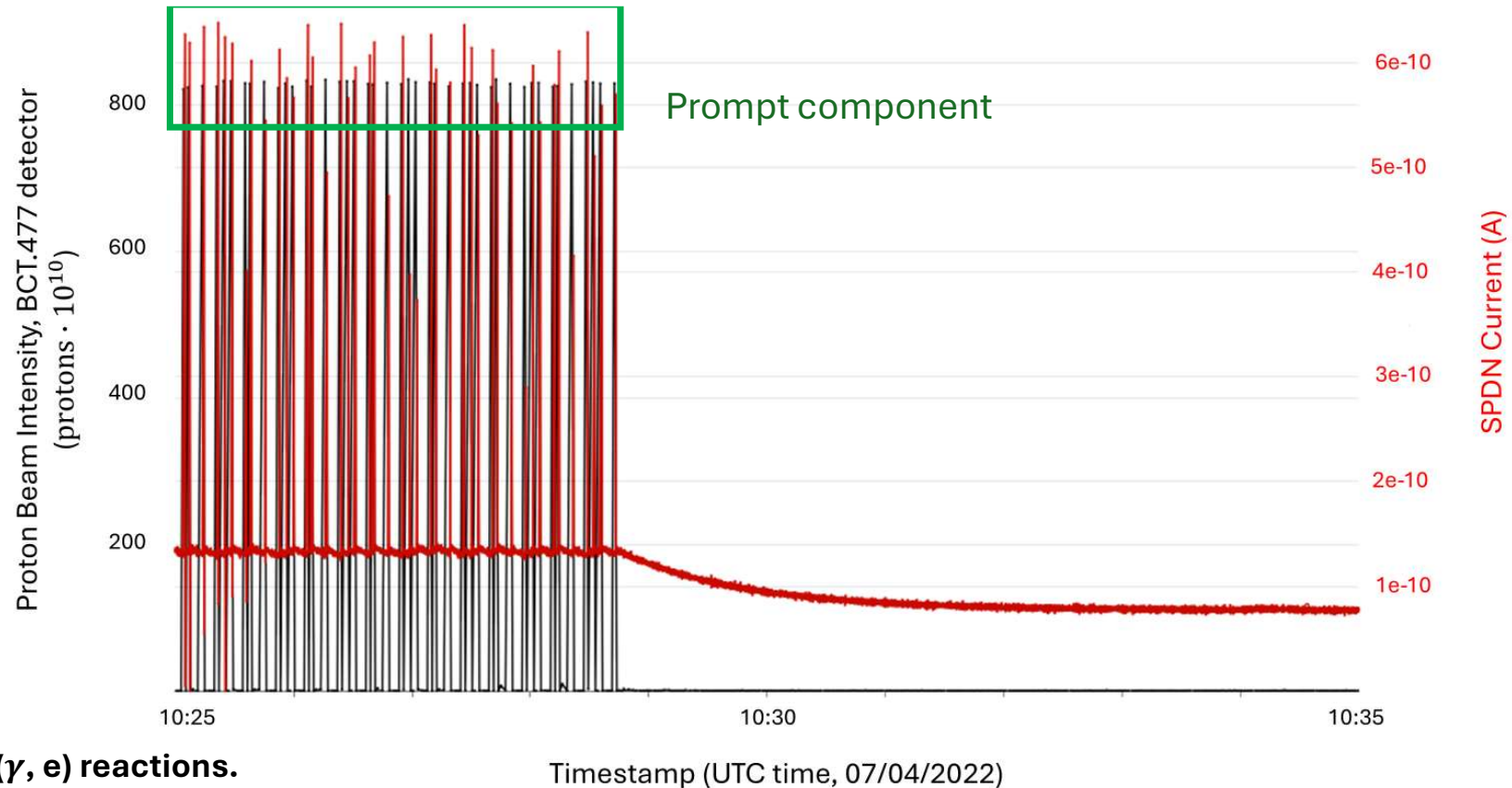
Left side **Rh and V detectors** show only a ~**35-45%** of the sensitivity of the right side.



Although the BCT.477 detector measures the same number of protons, the **neutron and gamma distribution on the target are different in both sides.**

4. Prompt Response Analysis: Methodology

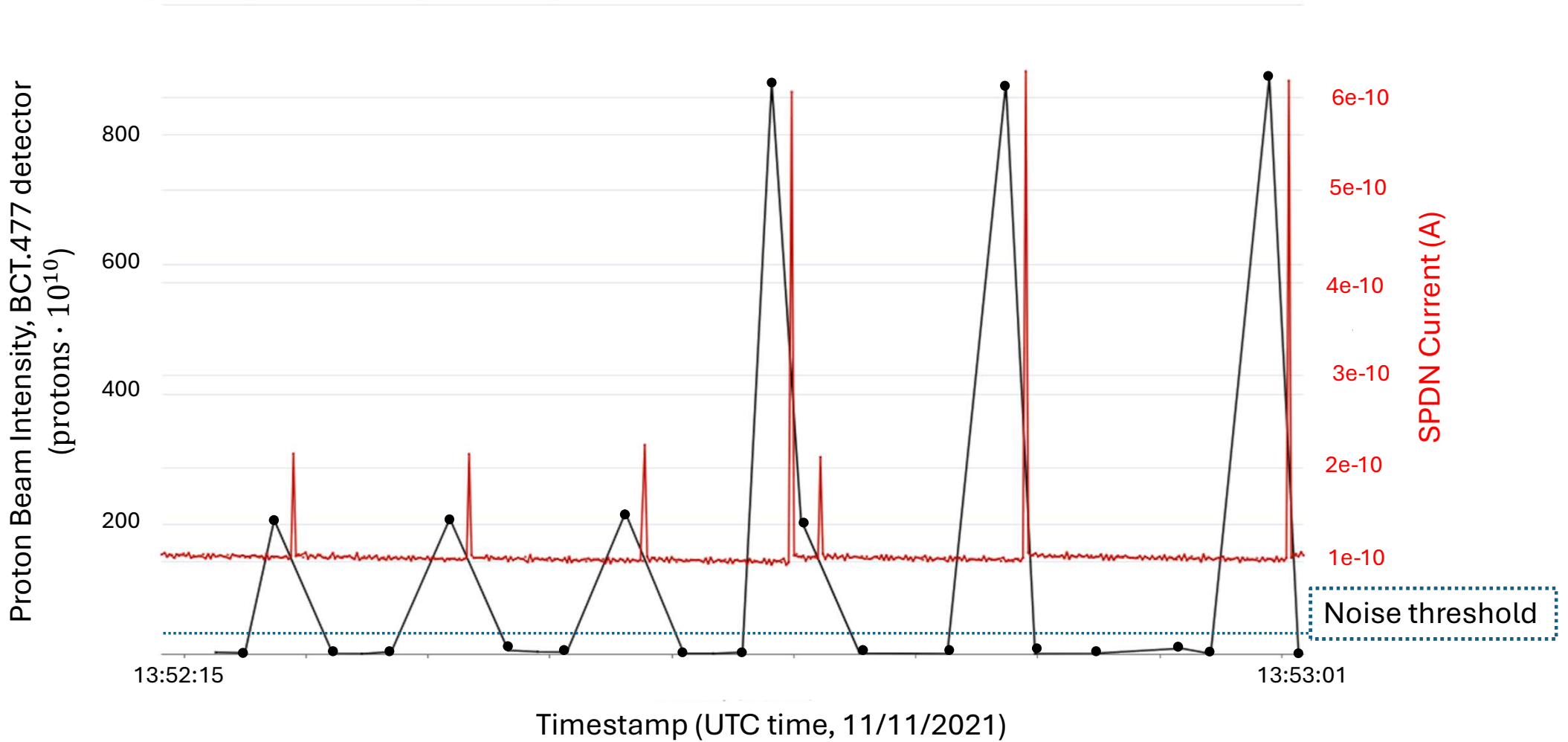
Prompt component analysis: Overview and Analysis



To analyze the data, the **peaks** are **separated** from the baseline, **subtracting** the local average of the peak, and the **relation to the peak of the beam** is calculated. The delay of the SPND peak respect to the beam peak is also calculated.

4. Prompt Response Analysis: Methodology

Prompt component analysis: Analysis



4. Prompt Response Analysis: Methodology

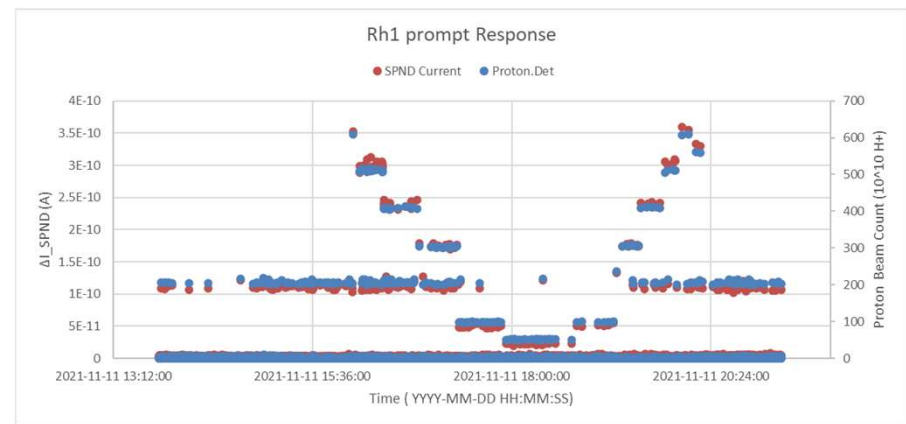
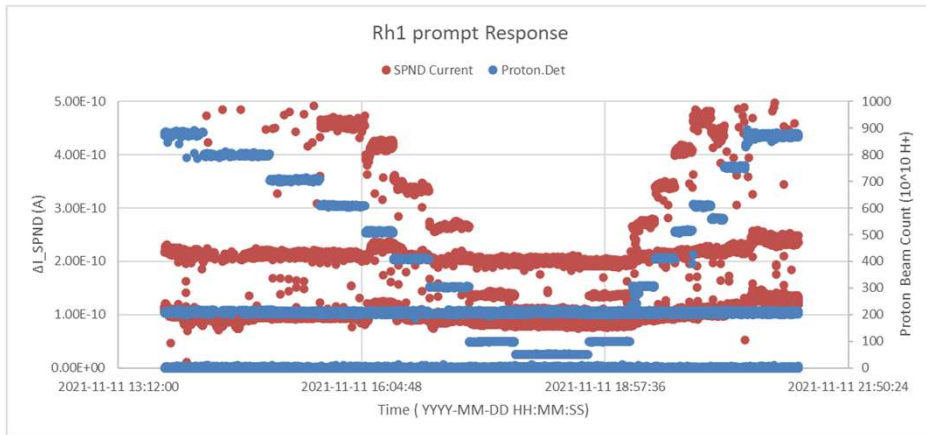
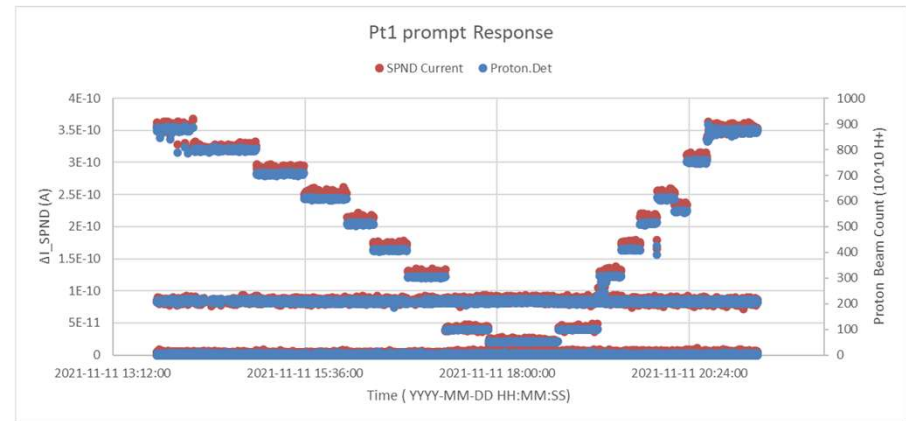
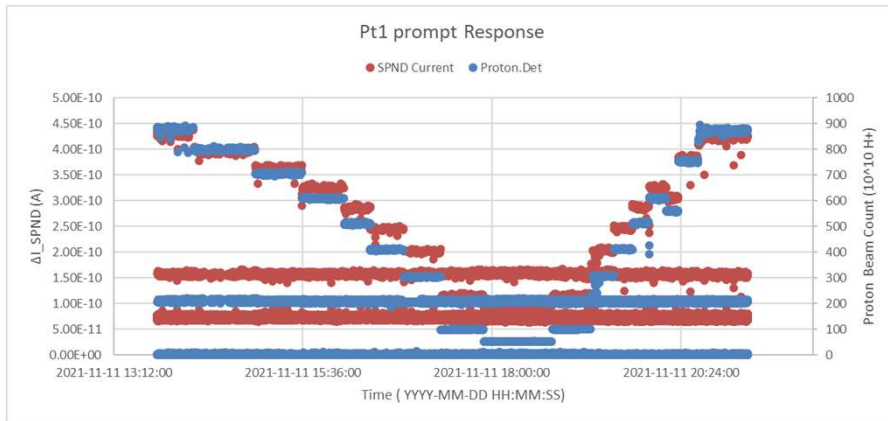
Prompt component analysis: Analysis

- Proton pulses under $40 \cdot 10^{10}$ protons have been skipped (noise)
- The median of the current measurements between the peaks of proton is found.
- If any value in the interval exceeds the median by a threshold value (THP) it is considered outside of the baseline and it is marked as a maximum:
 - THP = 8% except for the SPND rhodium 1 whose THP = 2% due to the high background noise.
- The intervals that contain 2 or more maxima are omitted.
- Excluding the maxima, the average of the rest of values is considered as the baseline.
- The increment of the SPND current in the interval is calculated by subtracting the baseline from the maxima.

stamp (UTC)	Timestamp (UTC TIME)	N.BCT.477:TOTAL INTENS	SPND Rh1-L CURRENT
13:45:07	45:06.7		7.463E-11
13:45:07	45:06.7	884.4359	
13:45:07	45:06.8		7.507E-11
13:45:07	45:06.9		7.315E-11
13:45:07	45:07.0		7.387E-11
13:45:07	45:07.1		7.763E-11
13:45:07	45:07.2		7.164E-11
13:45:07	45:07.3		7.772E-11
13:45:07	45:07.4		7.313E-11
13:45:07	45:07.5		2.019E-10
13:45:08	45:07.6		7.717E-11
13:45:08	45:07.7		7.076E-11
13:45:08	45:07.8		7.656E-11
13:45:08	45:07.9		7.557E-11
13:45:08	45:07.9	1.0989	
13:45:08	45:08.0		7.402E-11
13:45:08	45:08.1		7.612E-11
13:45:08	45:08.2		7.164E-11
13:45:08	45:08.3		7.706E-11
13:45:08	45:08.4		7.509E-11
13:45:08	45:08.5		7.267E-11
13:45:09	45:08.6		7.624E-11
13:45:09	45:08.7		7.555E-11
13:45:09	45:08.8		7.271E-11
13:45:09	45:08.9		7.608E-11
13:45:09	45:09.0		7.284E-11
13:45:09	45:09.1		7.690E-11

4. Prompt Response Analysis: Results

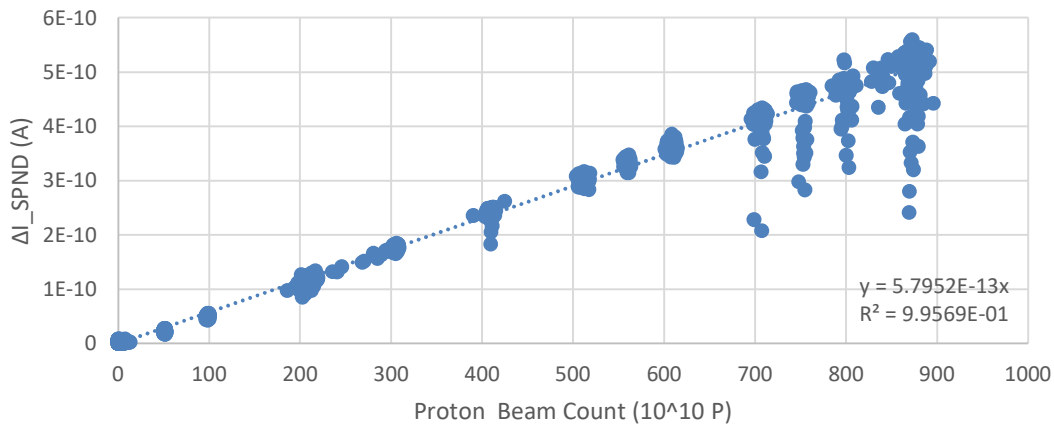
Prompt component analysis: Results



4. Prompt Response Analysis: Results

Prompt component analysis: Results

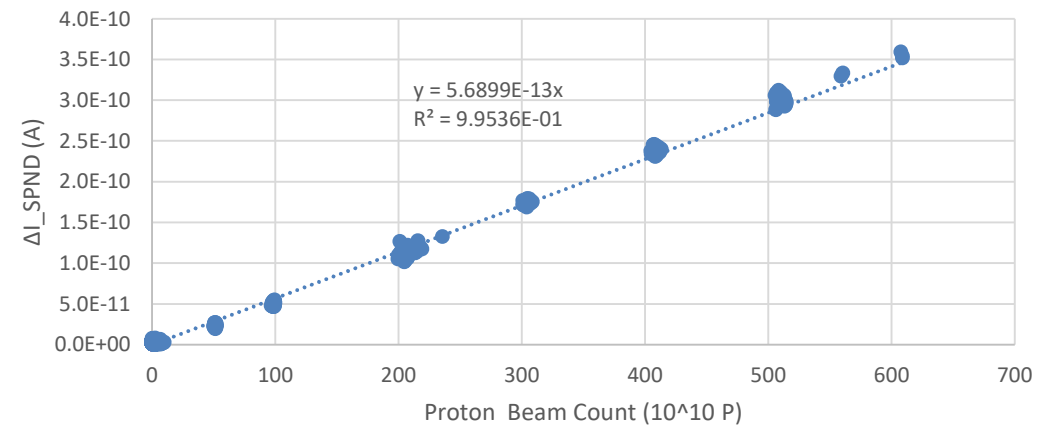
Rh1 prompt response (THP = 8%)



The sensitivity has been calculated as the slope of the linear fit, therefore:

$$S_p = \Delta I / N_p$$

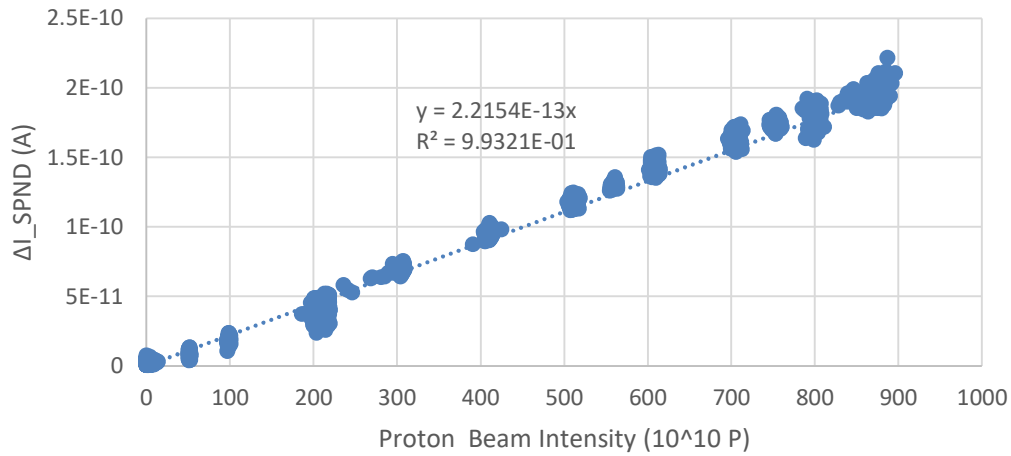
Pt1 prompt response (THP = 2%)



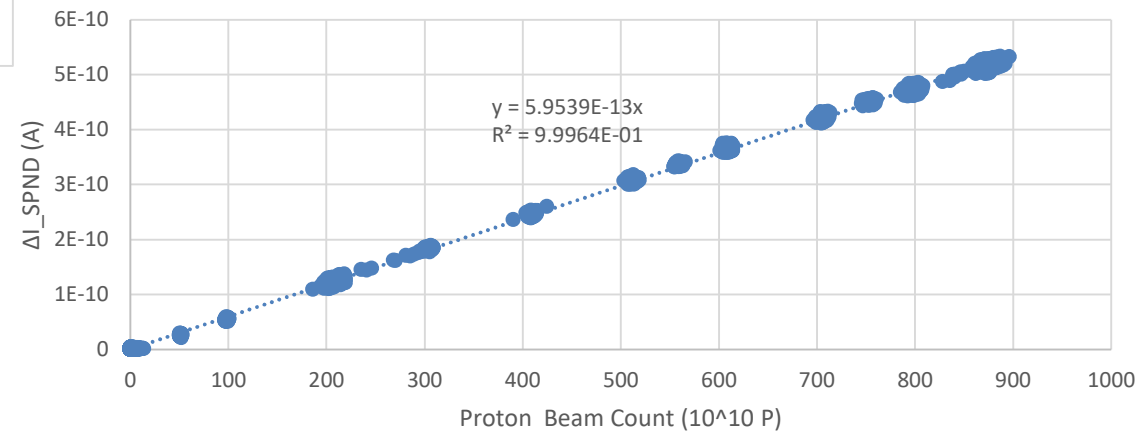
4. Prompt Response Analysis: Results

Prompt component analysis: Results

Co1 prompt response



Co2 prompt Response



4. Prompt Response Analysis: Results

Detector	S_p (AVG)	S_p (SD)	R^2	N_{samples}
Co_1	2.2154E-13	1.5E-16	0.9932	14378
Co_2	5.9539E-13	9E-17	0.9996	14361
Pt_1	4.097E-13	1E-16	0.9989	14154
Pt_2	8.028E-13	2.2E-16	0.9990	13242
Rh_1	5.690E-13	7E-16	0.9954	3311
Rh_2	6.361E-13	4E-16	0.9958	13198
V_1	1.3787E-13	1.7E-16	0.9801	13133
V_2	2.375E-13	6E-16	0.9974	459

SNPD type	Prompt Sensity (pA/P)		N
	Avg	SD	
Co	4.1E-13	2.6E-13	2
Pt	6.1E-13	2.8E-13	2
Rh	6.0E-13	4.7E-14	2
V	1.9E-13	7.0E-14	2

5. Conclusions

- The Rh-SPNDs presents a higher delayed sensitivity higher than V-SPNDs, about 13 to 15.
- The Pt SPNDs present the highest prompt sensitivity (between a 35 to 85%) higher than the rest of SPNDs.
- The prompt sensitivity of the Rh-SPND results higher than Co-SPNDs, that was surprising due to the Rh-SPNDs are mainly delayed detectors.
- According to the results the Rh-SPND could be the most versatile detector due to its highest delayed response and an almost the highest prompt sensitivity.
- According to the experimental results, at least some of the detectors appear to be good candidates for implementation in the STUMM module (IFMIF-DONES). Among them, the Rh detector exhibited the highest sensitivity to the neutron flux in the delayed component, as well as the strongest correlation with protons in the prompt response, making it the most promising detector so far.

6. Current and future tasks

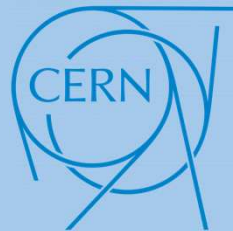
- To quantify the neutron fluency when the specification of the SPNDs were known
- Cross validation of the experimental data and the simulation when the numerical results and the exact placement of the SPNDs was known.
- To write a joint publication

Study of SPNDs irradiation at NEAR-nTOF (CERN): Data analysis



UNIVERSIDAD
DE GRANADA

Juan Antonio Moreno
Antonio Pousibet Garrido
Alberto J. Palma, ajpalma@ugr.es
Miguel Ángel Carvajal, carvajal@ugr.es



Salvatore Fiore
Ana-Paula Bernardes
Marco Calviani

Ciemat

Santiago Becerril
Rafael Vila